Control of Aircraft Landing using the Dynamic Inversion and the H-inf Control

Mihai Lungu*, Romulus Lungu*, Dragoş Tutunea**
*University of Craiova, Faculty of Electrical Engineering, Craiova, Romania
**University of Craiova, Faculty of Mechanics, Craiova, Romania
Lma1312@yahoo.com, romulus_lungu@yahoo.com, dragostutunea@yahoo.com

***Abstract* — The paper focuses on the automatic control of aircraft in the longitudinal plane, during landing, by using the literalized dynamics of aircraft, taking into consideration the wind shears and the errors of the sensors. The H-inf control provides robust stability with respect to the uncertainties caused by different disturbances and noise type signals, while the dynamic inversion provides good precision tracking. A new robust automatic landing system (ALS) is obtained by means of the H-inf control, the dynamic inversion, optimal observers, a dynamic compensator and two reference models providing the aircraft desired velocity and altitude. The theoretical results are validated using numerical simulations for a light aircraft landing; the simulation results are very good (Federal Aviation Administration accuracy requirements for Category III are met) and show the robustness of the algorithm even in the presence of wind shears and sensor errors.**

Keywords— landing; aircraft; H-inf control; dynamic inversion

I. INTRODUCTION

Many scientific researchers have applied the intelligent concepts for the automatic landing of aircraft; they use the optimal synthesis $H_2, H_\infty, H_2/H_\infty$ [1, 2], the adaptive synthesis based on dynamic inversion theory and neural networks theory [3, 4] or fuzzy techniques [5, 6]. In the research area of optimal synthesis, Ochi and Kanai [7] have used the H_∞ control technique to design aircraft automatic approach and landing. In this paper, the authors did not analyze the robustness of the designed controllers in the presence of sensor errors and wind shears – issue which is considered in our paper. This is achieved in [8], where a PD-type fuzzy control system is developed for automatic landing control of both linear and nonlinear aircraft models; the robustness for a wide range of initial conditions was demonstrated successfully [9]. The drawback is that the authors only set up the wind disturbance as the initial condition; persistent wind disturbance is not considered. The learning scheme using fuzzy controllers with the BPTT (Back-propagation Through Time), presented in [9], guides the aircraft to a safe landing and makes the controller more robust and adaptive to ever-changing environment. By using improvement calculation methods and high-accuracy instruments, these systems provide more accurate flight data to the ALS to make the landing smoother; however, these studies did not include weather factors such as wind disturbances [9]. Same conclusions can be drawn from the work of Singh and Padhi [10] where a nonlinear control has been designed using the dynamic inversion approach for the automatic landing of unmanned aerial vehicles (UAVs) along with associated path planning. The obtained algorithm is not tested in the presence of wind shears, this being a disadvantage of the algorithm. Other methods to design the control for aircraft landing involve the use of neural networks [11], but the weakness of these methods is that they do not make the aircraft to track the desired flight path with accuracy. If severe wind disturbances are encountered, the pilot must handle the aircraft due to the limits of the automatic landing system.

This paper focuses on the automatic control of aircraft in the longitudinal plane, during landing, using the aircraft linearized longitudinal dynamics, taking into consideration the errors of the sensors as well as the longitudinal and vertical wind shears. Our aim is to design a new landing control system in the longitudinal plane by using the H-inf control and the dynamic inversion concept. The controlled output vector (z) consists of the aircraft flight altitude and velocity, the disturbances of the system being the wind shears and the sensor measurement errors. The reference altitude, velocity, and their derivatives up to relative degrees of the system are provided by reference models by means of the landing geometry equations [12, 13]. The system differs from other similar automatic landing systems from the specialty literature. Our new automatic landing system consists of: 1) an optimal observer – used for the estimation of a state error vector in the presence of wind shears and sensor errors; 2) two reference models providing the desired altitude and velocity on the landing trajectory, together with the derivatives of these variables up to the relative degree of the system; 3) a dynamic compensator which provides one of the control law components (the pseudo-command signal). The inputs of the reference models are the altitude and the velocity calculated by using the landing geometry equations for the two main stages of the landing (glide slope and flare).

II. AIRCRAFT DYNAMICS IN LONGITUDINAL PLANE

The linearized dynamics used in this paper belongs to a light aircraft (Charlie-1 type) flight. The dynamics of aircraft motion, in longitudinal plane, is described by the state equation [13]:

$$\dot{\boldsymbol{x}} = A\boldsymbol{x} + B\boldsymbol{u} + G\boldsymbol{u}_{\boldsymbol{w}}, \tag{1}$$

with $\boldsymbol{x} \in R^{7\times 1}$ – state vector, $\boldsymbol{x} = \begin{bmatrix} u & w & q & \theta & H & \delta_e & \delta_T \end{bmatrix}^T$, $\boldsymbol{u} = \begin{bmatrix} \delta_{ec} & \delta_{Tc} \end{bmatrix}^T \in R^{2\times 1}$ – control vector, while $\boldsymbol{u}_{\boldsymbol{w}} = \begin{bmatrix} V_{vx} & V_{vz} \end{bmatrix}^T$ is the vector of disturbances; V_{vx} and V_{vz} are the components of the wind velocity along the aircraft longitudinal and vertical [1]; u is the longitudinal velocity, w – vertical velocity, q – pitch angular rate, θ – pitch angle, H – aircraft altitude, while δ_e and

δ_T are the elevator deflection and the thrust command, respectively; δ_{ec} and δ_{Tc} are the commands applied to elevator and engine, respectively. The matrices $A \in R^{7\times7}, B \in R^{7\times2}$ and $G \in R^{7\times2}$ are, respectively [13]:

$$A=\begin{bmatrix} a_{11} & a_{12} & 0 & a_{14} & 0 & b_{11} & b_{12} \\ a_{21} & a_{22} & a_{23} & 0 & 0 & b_{21} & b_{22} \\ a_{31} & a_{32} & a_{33} & 0 & 0 & b_{31} & b_{32} \\ 0 & 0 & 1 & 0 & 0 & 0 & 0 \\ 0 & a_{52} & 0 & a_{54} & 0 & 0 & 0 \\ 0 & 0 & 0 & 0 & 0 & -1/T_e & 0 \\ 0 & 0 & 0 & 0 & 0 & 0 & -1/T_T \end{bmatrix}, B=\begin{bmatrix} 0 & 0 \\ 0 & 0 \\ 0 & 0 \\ 0 & 0 \\ 0 & 0 \\ 1/T_e & 0 \\ 0 & 1/T_T \end{bmatrix}, G=\begin{bmatrix} -a_{11} & -a_{12} \\ -a_{21} & -a_{22} \\ -a_{31} & -a_{32} \\ 0 & 0 \\ 0 & 0 \\ 0 & 0 \\ 0 & 0 \end{bmatrix}. \quad (2)$$

The landing procedure involves three phases: initial approach, glide slope, and flare [14, 15]. During initial approach, the pilot descends from the cruise altitude to 420 m above the ground. At 4 nautical miles from the runway, the glide slope path signal is intercepted; the pitch, attitude and speed must be controlled while the aircraft maintains a constant speed; the pitch angle is between -5 and 5 deg. At 30 m above the ground, the slope angle control system is disengaged and a flare maneuver is executed.

The equation associated to the glide slope phase ($H \geq H_0$, $H_0 -$ the altitude at which the glide slope phase ends) is $H_c = \left(X - X_{p_0}\right)\tan\left(\gamma_c\right), \dot{X} = u\cos\theta + w\sin\theta,$ where X is the covered horizontal distance, X_{p_0} is the coordinate of the point where the glide slope intersects the horizontal axis, $H_c -$ the calculated flight altitude, while $\gamma_c = -2.5\,\text{deg}$ is the imposed slope angle during the first landing stage. The equation associated to the flare is $H_c = H_0 \exp\left(-t/\tau\right)$, with $\tau -$ time constant. In (1) $\boldsymbol{u}_w$ is a stochastic process defined by means of the velocities' spectrum; the velocities may be modeled using generator filters [9] with white noise input type. Here, the disturbances are the wind shears, their model being described by the equations [1]: $V_{vx} = -V_{vx_0}\sin\left(\omega_0 t\right), V_{vz} = -V_{vz_0}\left[1-\cos\left(\omega_0 t\right)\right], \omega_0 = 2\pi/T_0,$ where T_0 is the flight time period inside the wind shear, while V_{vx_0} and V_{vz_0} are the maximum absolute values of the wind velocities with respect to longitudinal and vertical axes, respectively.

III. Design of the Automatic Landing System by using the Dynamic Inversion and the H-inf Control Method

In this section of the paper, the automatic landing system is designed. It is based on the dynamic inversion principle and H-inf method, a dynamic compensator being used in the design process of the component $\overline{\boldsymbol{u}}$ of the control law *u*. The automatic landing system is more appropriate for the cases when aircraft dynamics is strongly nonlinear. For the calculation of the command $\boldsymbol{u}_\infty$, an optimal H-inf based procedure is used.

A. Problem formulation

Consider the vector $z = \begin{bmatrix} H & u \end{bmatrix}^T = C'\boldsymbol{x}$ that contains the system controllable output variables, while the vector $\bar{z} = \begin{bmatrix} \overline{H} & \overline{u} \end{bmatrix}^T$ contains the reference variables (the imposed values of the flight altitude and longitudinal velocity). The system output vector (*y*), in the absence of sensor errors, has the form: $y = \begin{bmatrix} H & \dot{H} & u & \dot{u} & \theta & q \end{bmatrix}^T = C\boldsymbol{x}$. If the sensor errors are taken into account, the output vector is $y = C\boldsymbol{x} + D_{22}e$, where *e* is the vector containing the sensor errors, while D_{22} is a positive defined matrix; the forms of the vector *e* and matrix D_{22} will be presented later. Having in mind the forms of the vectors $\boldsymbol{x}$, $\boldsymbol{u}$, $\boldsymbol{u}_w$, and the matrices *A*, *B*, *G* - equations (2), it results:

$$C'=\begin{bmatrix} 0 & 0 & 0 & 0 & 1 & 0 & 0 \\ 1 & 0 & 0 & 0 & 0 & 0 & 0 \end{bmatrix}, C=\begin{bmatrix} 0 & 0 & 0 & 0 & 1 & 0 & 0 \\ 0 & a_{52} & 0 & a_{54} & 0 & 0 & 0 \\ 1 & 0 & 0 & 0 & 0 & 0 & 0 \\ a_{11} & a_{12} & 0 & a_{14} & 0 & b_{11} & b_{12} \\ 0 & 0 & 0 & 1 & 0 & 0 & 0 \\ 0 & 0 & 1 & 0 & 0 & 0 & 0 \end{bmatrix}. \quad (3)$$

Now, by using $\bar{z}$ and the dynamic inversion principle, we calculate $\bar{x}$ (the desired state of the system) and $\overline{\boldsymbol{u}}$ (the desired control) with respect to $\bar{z}$ and, after that, the vector $\bar{y}$ is obtained with the equations: $\dot{\bar{x}} = A\bar{x} + B\overline{\boldsymbol{u}}, \bar{z} = C'\bar{x}, \bar{y} = C\bar{x}$.

The command law is calculated by using the formula [13]:

$$\boldsymbol{u} = \boldsymbol{u}_\infty + \overline{\boldsymbol{u}}, \quad (4)$$

where $\boldsymbol{u}_\infty$ is the optimal command calculated by means of the H-inf method, while the component $\overline{\boldsymbol{u}}$ is calculated by using the dynamic inversion. We present below the calculation of the two components of the control law.

B. Design of the first component of the control law

If the state equation (1), the equations of the variables $z_1 = H, z_2 = u,$ and the equation $y = C\boldsymbol{x} + D_{22}e$ are put together, the following equation is obtained:

$$\begin{bmatrix} \dot{\boldsymbol{x}} \\ z_1 \\ z_2 \\ y \end{bmatrix} = \begin{bmatrix} A_{(7\times7)} & B_{(7\times2)} & G_{(7\times2)} & 0_{(7\times6)} \\ C_{0(1\times7)} & D_{01(1\times2)} & 0_{(1\times2)} & 0_{(1\times6)} \\ C_{1(1\times7)} & D_{11(1\times2)} & 0_{(1\times2)} & 0_{(1\times6)} \\ C_{(6\times7)} & 0_{(6\times2)} & 0_{(6\times2)} & D_{22(6\times6)} \end{bmatrix} \begin{bmatrix} \boldsymbol{x} \\ \boldsymbol{u} \\ \boldsymbol{u}_w \\ e \end{bmatrix}; \quad (5)$$

$C_0 = \begin{bmatrix} 0 & 0 & 0 & 0 & 1 & 0 & 0 \end{bmatrix}, C_1 = \begin{bmatrix} 1 & 0 & 0 & 0 & 0 & 0 & 0 \end{bmatrix}, D_{01} = \begin{bmatrix} c_1 & 0 \end{bmatrix}$ $D_{11} = \begin{bmatrix} c_2 & 0 \end{bmatrix}$, the matrix *C* has the form (3), c_1 and c_2 are positive constants, while $D_{22} = k \cdot I_6$ is the weights' matrix for the sensor errors' vector: $e = \begin{bmatrix} e_H & e_{\dot{H}} & e_u & e_{\dot{u}} & e_\theta & e_q \end{bmatrix}^T$; *k* is a small positive constant.

The optimal control law has the form [13]: $\boldsymbol{u}_\infty = -K_\infty\left(\hat{\boldsymbol{x}} - \bar{\boldsymbol{x}}\right),$ $K_\infty = R_1^+ B^T P_\infty, R_1 = D_{11}^T D_{11};$ K_∞ is the controller gain matrix, while $\boldsymbol{u}_\infty$ minimizes the cost functional:

$$J = \frac{1}{2}\int_0^\infty z_2^T z_2 \mathrm{d}t = \frac{1}{2}\int_0^\infty \left[\boldsymbol{x}^T \underbrace{\left(C_1^T C_1\right)}_{Q_1}\boldsymbol{x} + \boldsymbol{u}_\infty^T \underbrace{\left(D_{11}^T D_{11}\right)}_{R_1}\boldsymbol{u}_\infty\right]\mathrm{d}t. \quad (6)$$

The symmetric and positive defined matrix $P_\infty \in R^{7\times7}$ is the solution of the Riccati matriceal equation [6, 13]:

$$A^T P_\infty + P_\infty A - P_\infty \left(BR_1^{-1}B^T - \mu_1^{-2}GG^T\right)P_\infty + Q_1 = 0. \quad (7)$$

To obtain the system estimated state $(\hat{\boldsymbol{x}})$ and $\Delta\hat{\boldsymbol{x}} = \hat{\boldsymbol{x}} - \overline{\boldsymbol{x}}$, we use the observer [13]: $\Delta\dot{\hat{\boldsymbol{x}}} = A\Delta\hat{\boldsymbol{x}} + B\boldsymbol{u} + L_\infty\left(\Delta y - C\Delta\hat{\boldsymbol{x}}\right)$. The observer gain matrix $L_\infty \in R^{7\times 6}$ is calculated by using the formula: $L_\infty = P_\infty^* C^T\left(D_{22}^T D_{22}\right)^{-1}$, with P_∞^* – the solution of the Riccati matriceal equation [6, 13]:

$$AP_\infty^* + P_\infty^* A^T - P_\infty^*\left(C^T C - \mu_2^{-2}Q_1\right)P_\infty^* + GG^T = 0. \quad (8)$$

C. Design of the second component of the control law

The calculation procedure of the control law's second component ($\overline{\boldsymbol{u}}$) starts from the general equation associated to the aircraft linear or nonlinear dynamics: $\dot{\boldsymbol{x}} = f\left(\boldsymbol{x},\overline{\boldsymbol{u}}\right), z = h\left(\boldsymbol{x}\right)$, which is given by the hypothesis in [13]:

$$z^{(r)} = h_r\left(\boldsymbol{x},\overline{\boldsymbol{u}}\right), h_r = \frac{\mathrm{d}^r h}{\mathrm{d}t^r} = h^{(r)}, \frac{\partial h_i}{\partial \boldsymbol{u}} = 0, i = \overline{0,r}, \frac{\partial h_r}{\partial \boldsymbol{u}} \neq 0; \quad (9)$$

equation (9) states that all the derivatives $z^{(i)} = h_i\left(\boldsymbol{x},\overline{\boldsymbol{u}}\right) = h^{(i)}$, $i = \overline{0,r}$, do not depend on $\overline{\boldsymbol{u}}$ (the control law's first component), while $z^{(r)} = h_r\left(\boldsymbol{x},\overline{\boldsymbol{u}}\right) = h^{(r)}$ depends on $\overline{\boldsymbol{u}}$; r is the relative degree of the system. In this case, the vector containing the main controlled variables is $z = \begin{bmatrix} H & u \end{bmatrix}^T = \begin{bmatrix} h_1(\boldsymbol{x}) & h_2(\boldsymbol{x}) \end{bmatrix}^T$; also, $z^{(r)} = \begin{bmatrix} z_1^{(r_1)} & z_2^{(r_2)} \end{bmatrix}^T = \begin{bmatrix} \ddot{H} & \ddot{u} \end{bmatrix}^T = \begin{bmatrix} h_1^{(r_1)}(\boldsymbol{x}) & h_2^{(r_2)}(\boldsymbol{x}) \end{bmatrix}^T$.

Let $\hat{h}_r\left(\boldsymbol{x},\hat{\boldsymbol{u}}\right)$ be the best approximation of the function $h_r\left(\boldsymbol{x},\overline{\boldsymbol{u}}\right)$; our aim is to design the pseudo-control control law:

$$\hat{v} = h_r\left(z,\hat{\boldsymbol{u}}\right) \quad (10)$$

which interferes in the expression of the component $\overline{\boldsymbol{u}}$. The equations (9) and (10) are equivalent with:

$$\overline{\boldsymbol{u}} = h_r^{-1}\left(z,v\right), \hat{\boldsymbol{u}} = \hat{h}_r^{-1}\left(z,v\right); \quad (11)$$

if $\hat{h}_r = h_r$, then, according to the equations (9) and (10), it results: $z^{(r)} = v = \hat{v}$; otherwise,

$$z^{(r)} = \hat{v} + \varepsilon, \quad (12)$$

where $\varepsilon = h_r\left(z,\overline{\boldsymbol{u}}\right) - \hat{h}_r\left(z,\hat{\boldsymbol{u}}\right)$ is the approximation error of the function h_r (the inversion error) which can be seen as a disturbance of the system. Equation (12) expresses the presence of *r* ideal integrators between the pseudo-control *v* and the output *z*. Imposing $z \to \overline{z}, \dot{z} \to \dot{\overline{z}}, \ldots, z^{(r)} \to \overline{z}^{(r)}$, the pseudo-control *v* may be chosen of the following form [13]: $v = \hat{v} + \varepsilon = \overline{z}^{(r)} + \hat{v}_{pd} + \varepsilon$, where $\hat{v}_{pd}$ is the output of the dynamic compensator (used for the stabilization of the dynamics (12)). The linear subsystem (12), having the input $v = \hat{v} + \varepsilon$ and the output *z*, has the transfer matrix $H_d(\mathrm{s}) = \begin{bmatrix} H_{d_1}(\mathrm{s}) & H_{d_2}(\mathrm{s}) \end{bmatrix}^T$, with $H_{d_i}(\mathrm{s}), i = \overline{1,2}$, having the form:

$$H_{d_i}(\mathrm{s}) = \frac{b_{0_i}}{\mathrm{s}^{r_i} + \lambda_{r_i-1,i}\mathrm{s}^{r_i-1} + \ldots + \lambda_{1,i}\mathrm{s} + \lambda_{0,i}}. \quad (13)$$

Now, by using the notations: $Z = \begin{bmatrix} z & \dot{z} & \ldots & z^{(r-1)} \end{bmatrix}^T =$

$= \begin{bmatrix} z_1 & \dot{z}_1 & \ddot{z}_1 & z_2 & \dot{z}_2 \end{bmatrix}^T = \begin{bmatrix} H & \dot{H} & \ddot{H} & u & \dot{u} \end{bmatrix}^T, \lambda = \begin{bmatrix} \lambda_1 & \lambda_2 \end{bmatrix}^T, \lambda_i =$

$= \begin{bmatrix} \lambda_{0,i} & \lambda_{1,i} & \ldots & \lambda_{r_i-1,i} \end{bmatrix}^T$, the subsystem (12) is written as:

$$z^{(r)} + \lambda^T Z = b_0\left(\hat{v} + \varepsilon\right), b_0 = \begin{bmatrix} b_{01} & b_{02} \end{bmatrix}^T. \quad (14)$$

Customizing the above equation for $z^{(r)} = \overline{z}^{(r)}$, the error $\varepsilon = \begin{bmatrix} \varepsilon_1 & \varepsilon_2 \end{bmatrix}^T$ becomes $\begin{bmatrix} 0 & 0 \end{bmatrix}^T$; for $b_0 = \begin{bmatrix} 1 & 1 \end{bmatrix}^T$, we obtain $\hat{v} = \hat{v}_r = \begin{bmatrix} \hat{v}_{r_1} & \hat{v}_{r_2} \end{bmatrix}^T$ and $\hat{v}_r = \overline{z}^{(r)} + \lambda\overline{Z} = \begin{bmatrix} \overline{\ddot{H}} + \lambda_{21}\overline{\ddot{H}} & \overline{\ddot{u}} \end{bmatrix}^T$. For $z_1 = H\,(r_1 = 3)$ and $z_2 = u\left(r_2 = 2\right)$, the following transfer functions result: $H_{d_1}(\mathrm{s}) = \frac{b_{01}}{\mathrm{s}^2\left(\mathrm{s} + \lambda_{21}\right)}, H_{d_2}(\mathrm{s}) = \frac{b_{02}}{\mathrm{s}^2}$, this leading to null stationary errors $\left(H_{st} = \dot{H}_{st} = u_{st} = \dot{u}_{st} = 0\right)$.

The left side term in equation (14) has now the expression:

$$z^{(r)} + \lambda^T Z = \begin{bmatrix} \dddot{H} + \ddot{H} \\ \ddot{u} \end{bmatrix} = \begin{bmatrix} a_{51}'' & a_{52}'' & a_{53}'' & a_{54}'' & 0 & a_{56}'' & a_{57}'' \\ a_{11}' & a_{12}' & a_{13}' & a_{14}' & 0 & a_{16}' & a_{17}' \end{bmatrix}\hat{\boldsymbol{x}} +$$
$$+ \begin{bmatrix} \frac{a_{52}b_{21}}{T_e} & \frac{a_{52}b_{22}}{T_T} \\ \frac{b_{11}}{T_e} & \frac{b_{12}}{T_T} \end{bmatrix}\hat{\boldsymbol{u}} + \begin{bmatrix} \overline{g}_{51}' & \overline{g}_{52}' \\ g_{11}' & g_{12}' \end{bmatrix}\boldsymbol{u}_{\boldsymbol{w}} + \begin{bmatrix} g_{51}'' & g_{52}'' \\ g_{11} & g_{12} \end{bmatrix}\dot{\boldsymbol{u}}_{\boldsymbol{w}}, \quad (15)$$

with $a_{51}'' = a_{51}' + a_{52}a_{21}, a_{52}'' = a_{51}' + a_{52}a_{22}, a_{53}'' = a_{53}' + a_{54} + a_{52}a_{23}$,

$a_{54}'' = a_{54}', a_{56}'' = a_{56}' + g_{21}, a_{57}'' = a_{57}' + g_{22}, \overline{g}_{51}' = g_{51}' + g_{21}$,

$\overline{g}_{52}' = g_{52}' + g_{22}$; we have chosen $\lambda_{21} = b_{01} = 1$.

Introducing $z^{(r)} + \lambda^T Z$ (the form is given in equation (15)) into equation (14) and identifying the terms of the pseudo-control $\hat{v}$ and ε, we get: $\hat{v} = \begin{bmatrix} \hat{v}_1 \\ \hat{v}_2 \end{bmatrix} = \begin{bmatrix} \hat{h}_{r_1}\left(z,\hat{\boldsymbol{u}}\right) \\ \hat{h}_{r_2}\left(z,\hat{\boldsymbol{u}}\right) \end{bmatrix} = \hat{h}_r\left(\hat{H},\hat{u},\hat{\boldsymbol{u}}\right)$,

$\hat{\boldsymbol{u}} = \begin{bmatrix} \hat{\delta}_{ec} & \hat{\delta}_{Tc} \end{bmatrix}^T$; thus, it result $\hat{\boldsymbol{u}} = \begin{bmatrix} \hat{\delta}_{ec} & \hat{\delta}_{Tc} \end{bmatrix}^T = \hat{h}_r^{-1}\left(\hat{z},\hat{v}\right) =$

$$= \begin{bmatrix} \frac{a_{52}b_{21}}{T_e} & \frac{a_{52}b_{22}}{T_T} \\ \frac{b_{11}}{T_e} & \frac{b_{12}}{T_T} \end{bmatrix}^{-1}\left(\hat{v} - \begin{bmatrix} a_{51}'' & a_{11}' \end{bmatrix}\begin{bmatrix} \hat{H} & \hat{u} \end{bmatrix}^T\right) \text{ and}$$

$$\varepsilon = \begin{bmatrix} \varepsilon_1 \\ \varepsilon_2 \end{bmatrix} = \begin{bmatrix} a_{51}'' & a_{52}'' & a_{53}'' & a_{54}'' & 0 & a_{56}'' & a_{57}'' \\ a_{11}' & a_{12}' & a_{13}' & a_{14}' & 0 & a_{16}' & a_{17}' \end{bmatrix}\begin{bmatrix} \hat{u} & \hat{q} & \hat{\theta} & \hat{\delta}_e & \hat{\delta}_T \end{bmatrix}^T +$$
$$+ \begin{bmatrix} \overline{g}_{51}' & \overline{g}_{52}' \\ g_{11}' & g_{12}' \end{bmatrix}\boldsymbol{u}_{\boldsymbol{w}} + \begin{bmatrix} g_{51}'' & g_{52}'' \\ g_{11} & g_{12} \end{bmatrix}\dot{\boldsymbol{u}}_{\boldsymbol{w}}; \quad (16)$$

$\hat{H}$ and $\hat{u}$ are two of the seven components of the estimated state $\hat{\boldsymbol{x}}$, i.e. $\hat{H},\hat{u},\hat{w},\hat{q},\hat{\theta},\hat{\delta}_e,\hat{\delta}_T$. Also, using now the Taylor series of the function $h_r^{-1}\left(z,v\right)$, we successively obtain:

$\bar{\boldsymbol{u}} = h_r^{-1}(z,v) = \hat{h}_r^{-1}(z,\hat{v}) + \frac{\mathrm{d}}{\mathrm{d}v}\left(h_r^{-1}(z,v)\right)_{v=\hat{v}} \cdot (v-\hat{v}) = (v-\hat{v}) =$

$= \hat{h}_r^{-1}(z,\hat{v}) + \frac{\mathrm{d}}{\mathrm{d}\hat{v}}\left(\hat{h}_r^{-1}(z,\hat{v})\right)\cdot \varepsilon$ and, replacing the controlled vector z with its estimate $(\hat{z})$, according to (11), it results: $\bar{\boldsymbol{u}} = \hat{\boldsymbol{u}} + \varepsilon \frac{\mathrm{d}}{\mathrm{d}\hat{v}}\left(\hat{h}_r^{-1}(\hat{z},\hat{v})\right)$. Now, replacing $\hat{\boldsymbol{u}}$ in the previous equation, we obtain the following control law:

$$\bar{\boldsymbol{u}} = \begin{bmatrix} \bar{\delta}_{ec} \\ \bar{\delta}_{Tc} \end{bmatrix} = \hat{h}_r^{-1}(\hat{z},v) = \begin{bmatrix} \frac{a_{52}b_{21}}{T_e} & \frac{a_{52}b_{22}}{T_T} \\ \frac{b_{11}}{T_e} & \frac{b_{12}}{T_T} \end{bmatrix}^{-1} \left(v - \begin{bmatrix} a''_{51} & a'_{11} \end{bmatrix} \begin{bmatrix} \hat{H} & \hat{u} \end{bmatrix}^T \right). \quad (17)$$

The calculation method for $\bar{\boldsymbol{u}}$ differs from other methods by a greater degree of generality, applicability, and simplicity.

IV. Structure of the New Automatic Landing System

The structure of the new automatic landing system, using a dynamic compensator, the dynamic inversion principle, and the H-inf method is presented in Fig. 1; it uses the two reference models in Fig. 2 (the three order reference model for *H* and the second order reference model for *u*). The vectors $\hat{v}_r = \bar{z}^{(r)} + \lambda \bar{Z}$ and $\bar{z}$ are provided by the two reference models, while the calculated aircraft altitude (H_c) is obtained from the landing geometry equations: $H_c = (X - X_{p_0})\tan(\gamma_c)$ for glide slope and $H_c = H_0 \exp(-t/\tau)$ for the flare. The command $\hat{v}$ is obtained using the output $\hat{v}_r$ of the reference models block and the output $\hat{v}_{pd}$ of the dynamic compensator; this signal $(\hat{v}_{pd})$ is obtained by using the vectors $z = [H \quad u]^T, \bar{z} = [\bar{H} \quad \bar{u}]^T$, the proportional coefficients (k_{p_1}, k_{p_2}), and the derivative coefficients (k_{d_1}, k_{d_2}) of the dynamic compensator. For the calculation of the coefficients $k_{p_1}, k_{p_2}, k_{d_1}, k_{d_2}$, we use the characteristic equations associated to the closed loop system (with negative unitary feedback) which has on its direct way the linear system with the transfer matrix $H_d(\mathrm{s})$ and the dynamic compensator (the command signal $\boldsymbol{u}_\infty$ is neglected); these equations are:

$$\mathrm{s}^3 + \lambda_{21}\mathrm{s}^2 + b_{01}k_{d_1}\mathrm{s} + b_{01}k_{p_1} = 0, \mathrm{s}^2 + (b_{02}k_{d_2} + \lambda_{12})\mathrm{s} + b_{02}k_{p_2} = 0; \quad (18)$$

choosing $\lambda_{21} = b_{01} = b_{02} = 1$ and $\lambda_{12} = 0$, the 4 coefficients of the dynamic compensator are determined such that the solutions of the equations (18) have negative real parts. The solutions of the equations (18) may be chosen as the poles of the transfer functions associated to the reference models.

The obtaining of the aircraft desired trajectory mainly involves the same two variables' control: the forward speed (*u*) and the altitude (*H*); the ALS must also assure the convergences: $\Delta y \to 0 (y = C\boldsymbol{x} \to \bar{y} = C\bar{\boldsymbol{x}}), \Delta z \to 0, \Delta\hat{\boldsymbol{x}} \to 0 (\hat{\boldsymbol{x}} \to \boldsymbol{x} \to \bar{\boldsymbol{x}})$.

V. Numerical Simulation Results

To study the performances of the new obtained automatic landing system, we consider the landing of a Charlie-1 aircraft. Complex simulations in Matlab/Simulink environment have been performed; thus, we designed the optimal observer, the H-inf controller, the dynamic compensator and, after that, we validated the proposed automatic landing system. The values of the coefficients for aircraft dynamics have been borrowed from [12, 13]: $a_{11} = -0.021, a_{12} = 0.122, a_{14} = -0.322, a_{21} = -0.209,$ $a_{22} = -0.53, a_{23} = 2.21, a_{31} = 0.017, a_{32} = -0.164, a_{33} = -0.412,$ $a_{52} = -1, a_{54} = V_0 = 70\,\mathrm{m/s}, b_{11} = 0.01, b_{12} = 1, b_{21} = -0.064, b_{22} = -0.044,$ $b_{31} = -0.378, b_{32} = 0.544, T_e = 0.3\,\mathrm{s}, T_T = 2\,\mathrm{s}, \bar{u} = V_0, V_{vx0} = 5\,\mathrm{m/s},$ $V_{vz0} = 5\,\mathrm{m/s}, T_0 = 10\,\mathrm{s}$. The sensor errors' vector has been chosen as $e = [1\,\mathrm{m} \quad 1\,\mathrm{deg/s} \quad 1\,\mathrm{m} \quad 0\,\mathrm{m/s}^2 \quad 1\,\mathrm{deg} \quad 1\,\mathrm{deg/s}]^T$, while, for the reference models, we have chosen: $p = 25, \xi_1 = \xi_2 = 0.7,$ $\omega_1 = \omega_2 = 2\,\mathrm{rad/s}$. For first landing phase, we used the values: $H_p = H(0) = 420\,\mathrm{m}, X(0) = 0, X_{p_0} = -H_p / \tan(\gamma_c), \gamma_c = -2.5\,\mathrm{deg}.$ The initial value of the state vector has been chosen as: $\boldsymbol{x}(0) = [71\,\mathrm{m/s} \quad -7.1\,\mathrm{m/s} \quad -2\,\mathrm{grd/s} \quad -1\,\mathrm{deg} \quad 420\,\mathrm{m} \quad 1\,\mathrm{deg} \quad 0\,\mathrm{deg}]^T$. In order to obtain the proportional coefficients (k_{p_1}, k_{p_2}) and the derivative coefficients (k_{d_1}, k_{d_2}) of the dynamic compensator, the characteristic equations (18) are solved after replacing the complex number "s" with its desired values; we have chosen the set (-0.5, -1.2, -0.9) for the first characteristic equation and the set (-10, -1) for the second characteristic equation.

In Fig. 3 and Fig. 4 we represent the time characteristics for the glide slope landing phase and flare landing phase, respectively; the characteristics have been represented for the ALS affected by wind shears in the presence or in the absence of sensor errors (the sensors are used for the measurement of the states). The last four mini-graphics in Figs. 3 and 4 represent the deviations of the forward speed (*u*), sink rate $(\dot{H})$, slope angle (γ), and altitude (*H*), with respect to their nominal values, i.e. $u - \bar{u}, \dot{H} - \dot{\bar{H}}, \gamma - \gamma_c, H - \bar{H}$. The presence of the sensor errors is not visible: the curves with solid line (obtained for the ALS without sensor errors) overlap almost perfectly over the curves plotted with dashed line (obtained for the ALS with sensor errors). The time origin for the flare trajectory is chosen zero when the altitude is $H=H_0$=30 m (the altitude at which the glide slope phase ends). From last graphics in Figs. 3 and 4, we can see that the final error between the desired path and the actual path is less than 0.3 m during the glide slope phase and 0 for flare. These errors are very good if we analyze the Federal Aviation Administration (FAA) accuracy requirements for Category III (the best category); according to FAA Category III accuracy requirements, the vertical error (altitude deviation with respect to its nominal value) must be less than 0.5 m, while the final altitude at the end of flare must be 0 m. The reason that our design meets the requirement and achieves the design goal is that we used the H-inf robust control technique.

The problem of landing has also been discussed in other papers, different types of ALSs being designed [9, 10, 12-15]. If we make a brief comparison between our ALS and the ones based on an Instrumental Landing System or conventional/fuzzy control of flight altitude by using the system's state [12], we remark that from the system transient regime period and overshoot point of view, the ALS based on H-inf technique and

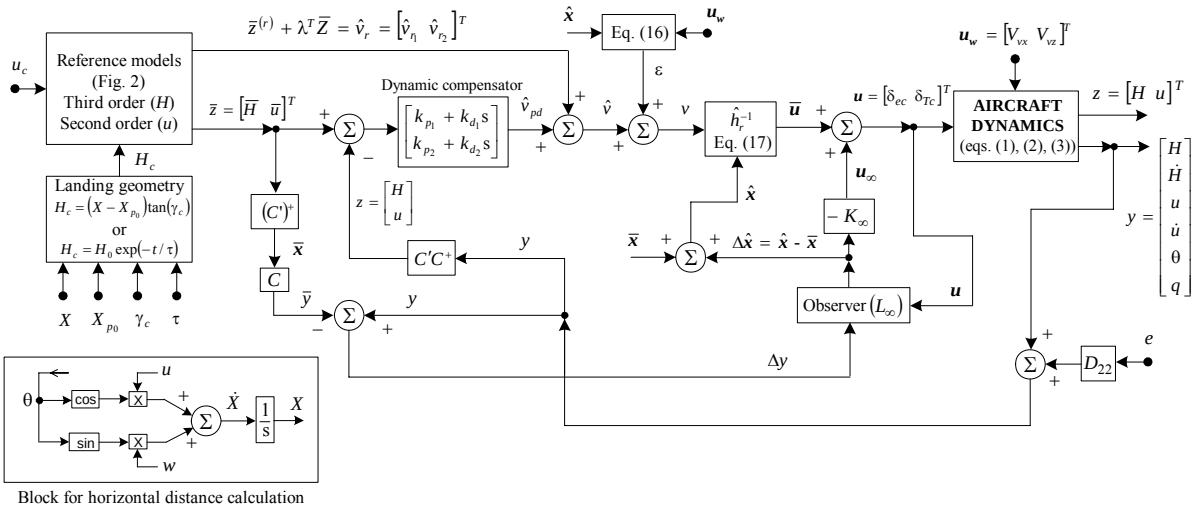

Fig. 1. New automatic landing system, using dynamic inversion and H-inf method

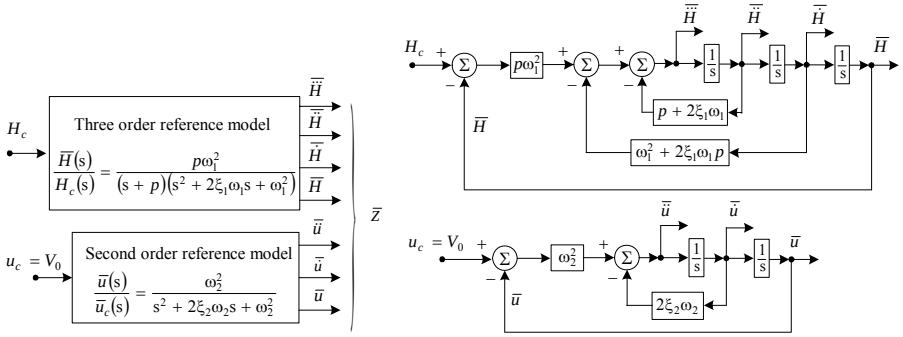

Fig. 2. Block diagrams of the three order and second order reference models, respectively: a) simplified block diagram; b) detailed block diagram

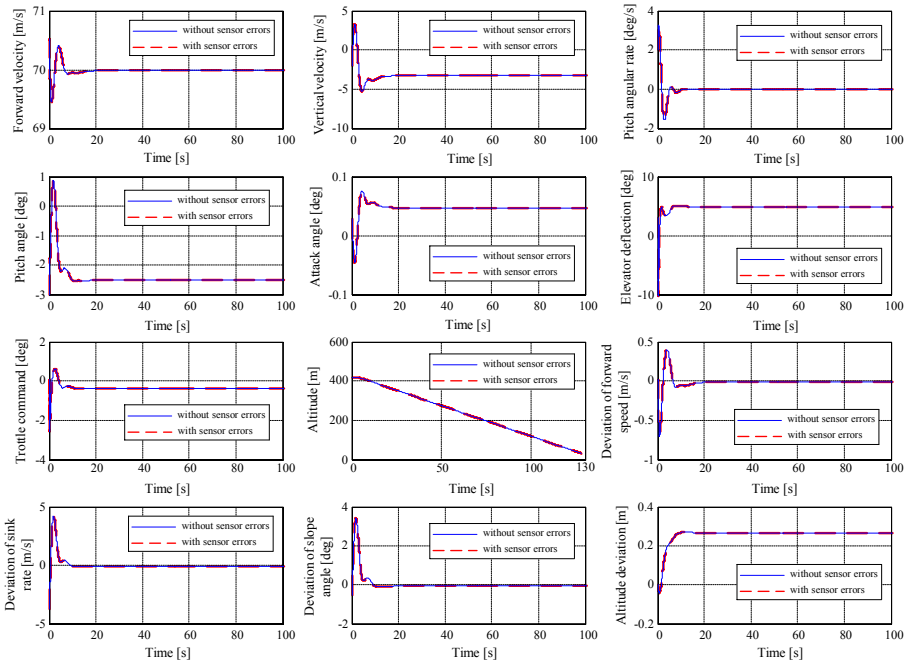

Fig. 3. Time characteristics for the glide slope phase

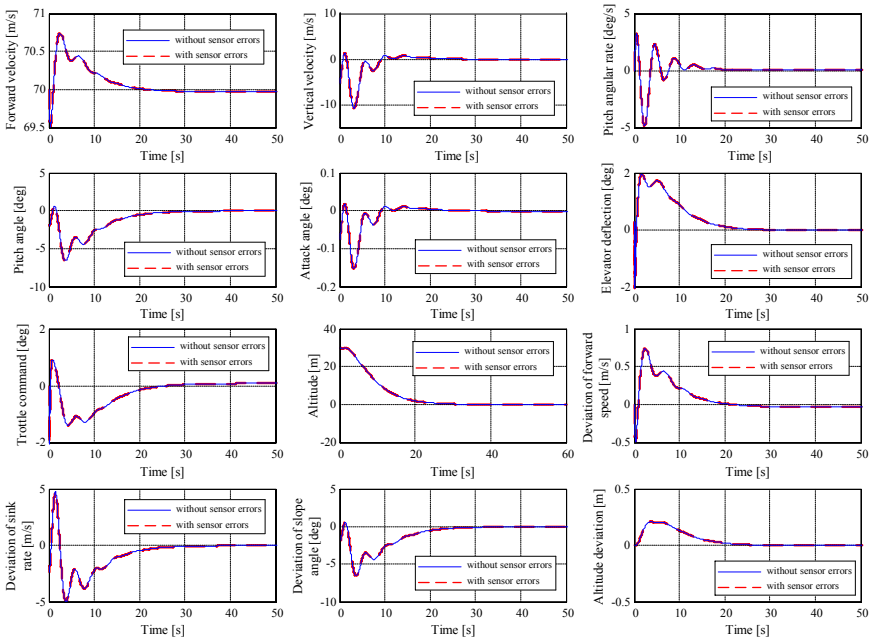

Fig. 4. Time characteristics for the flare phase

dynamic inversion works slightly better. Improvement of the performance was obtained by replacing the conventional controllers with fuzzy ones [14], but those ALSs cannot be used for strongly nonlinear dynamics. Our new ALS uses the H-inf technique, this having the advantage of applicability to problems involving multivariate systems with cross-coupling between channels; the only disadvantage is related to the non-linear constraints such as saturation that are generally not well-handled.

VI. Conclusion

The ALS designed in this paper represents an improved version of the one in [1] differing from other similar automatic landing systems from the specialty literature; our new ALS is designed for the control of landing in the longitudinal plane but, with some changes, it can be applied to the lateral-directional motion of the aircraft during landing or other flight trajectories. Our new ALS has some additional elements with respect to the one presented in [1]: an optimal observer, two reference models providing the desired altitude and velocity, and a dynamic compensator which provides one of the control law components. The simulation results are promising and show the robustness of the designed control system even in the presence of wind shears and sensor errors; moreover, the very good errors meet the FAA accuracy requirements for Category III. On the other hand, the designed control law has the ability to reject the measurement noise from sensors and wind shears having low intensity.

Acknowledgment

This work is supported by grant no. 89/1.10.2015 of the Romanian National Authority for Scientific Research and Innovation, CNCS-UEFISCDI, code PN-II-RU-TE-2014-4-0849.

References

[1] J. Che and D. Chen, "Automatic Landing Control using H-inf control and Stable Inversion," Proceedings of the 40th Conference on Decision and Control, Orlando, Florida, USA, pp. 241-246, 2001

[2] Y. Li, N. Sundararajan, and Z. Wang, "Robust neuro-H_∞ controller design for aircraft auto-landing," IEEE Transactions on Aerospace and Electronic Systems, vol. 40, no. 1, pp. 158-167, 2004.

[3] V. Kargin, "Design of An Autonomous Landing Control Algorithm for A fixed Wing UAV," M.S. Thesis, Ankara Technical University, 2007.

[4] H. Vo and S. Sridhar, "Robust Control of F-16 Lateral Dynamics," Int. Journal of Aerospace and Mechanical Engineering, pp. 80-85, 2008.

[5] V. Kumar, K. Rana, and V. Gupta, "Real-Time Performance Evaluation of a Fuzzy PI + Fuzzy PD Controller for Liquid-Level Process," International Journal of Intelligent Control and Systems, vol. 13, no. 2, pp. 89-96, 2008.

[6] S. Shue and R. Agarwal, "Design of automatic landing systems using mixed H_2/H_∞ control," Journal of Guidance, Control, and Dynamics, vol. 22, no. 1, pp. 103-114, 1999.

[7] Y. Ochi and K. Kanai, "Automatic approach and landing for propulsion controlled aircraft by H-inf control," Proceedings of the IEEE International Conference on Control Applications, Hawaii, pp. 997-1002, 1999.

[8] K. Nho and R. Agarwal, "ALS design using fuzzy logic," Journal of Guidance, Control and Dynamics, vol. 23, pp. 298-304, 2000.

[9] J. Juang and J. Chio, "Fuzzy modelling control for aircraft automatic landing system," Int. Journal of Systems Science, vol. 36, no. 2, pp. 77-87, 2005.

[10] S. Singh and R. Padhi, "Automatic Path Planning and Control Design for Autonomous Landing of UAVs using Dynamic Inversion," American Control Conference, St. Louis, MO, USA, 2409-2414, 2009.

[11] H. Afshari, J. Roshanian, and A. Novinzadeh, "Robust Nonlinear Optimal Solution to the Lunar Landing Guidance by using Neighboring Optimal Control," Journal of Aerospace Engineering, vol. 24, no. 1, pp. 20-30, 2011.

[12] R. Lungu, M., Lungu, and T.L. Grigorie, "ALSs with conventional and fuzzy controllers considering wind shears and gyro errors," Journal of Aerospace Engineering, vol. 26, no. 4, pp. 794-813, 2012.

[13] R. Lungu and M. Lungu, "Controlul automat al aeronavelor la aterizare (Aircraft automatic control during landing)," Sitech Publisher, 2015.

[14] R. Lungu, M., Lungu, and T.L. Grigorie, "Automatic control of aircraft in longitudinal plane during landing," IEEE Transactions on Aerospace & Electronic Systems, vol. 49, no. 2, pp. 1338-1350, 2013.

[15] R. Lungu and M. Lungu, "Automatic landing control using H-inf control and dynamic inversion," Proceedings of the Institution of Mechanical Engineers Part G Journal of Aerospace Engineering, vol. 228, no. 14, pp. 2612-2626, 2014.